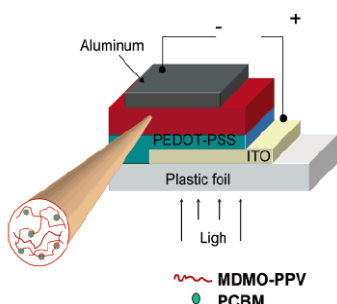


## Final Report: Recovery Act - Nano-composite Structures for OPV Devices

### 1. Introduction

Abundant for most of the year in most parts of the world, solar energy is the ultimate renewable zero-emission energy source. Combined with improved means of energy storage, it has the potential to supply a quickly increasing fraction of our energy needs. However, its widespread use for electricity generation requires a significant further decrease in cost, which will be difficult to meet with conventional crystalline silicon technology. Allowing for the use of inexpensive, high-speed, large-scale roll-to-roll manufacturing processes, organic photovoltaics



**Fig. 1** Bulk heterojunction configuration in organic solar cells (taken from <sup>10</sup>).

(OPV) have a significant chance of quickly becoming an essential factor in electricity generation<sup>1</sup>, but additional improvements in performance and life-time are needed before large-scale implementation. OPV devices, also called polymer-solar cells (PSC) or polymer-fullerene composite solar cells, are lightweight and can be flexible, opening the possibility for a range of new applications including large-area pliable devices<sup>2</sup>. While power-conversion efficiencies of up to 7.9% have been reported at a laboratory scale<sup>3,4</sup>, practical maximum efficiencies between 20 and 25% appear to be reasonable<sup>5</sup>. Nanoscale morphology has been identified

as an important factor in the optimization of OPV<sup>1,2,4,5,6</sup>. In addition to tuning the optical and electronic properties of the materials used for light harvesting, carrier generation, transport, and collection, control of the nanoscale morphology of the active layer can alone provide a clear path to power conversion efficiencies of >10%. Tandem devices can certainly dramatically improve overall efficiencies<sup>7,8</sup>, but taking into account their complexity, additional gains can and must be made in single-layer devices.

The most common and scalable design of OPV (shown in Fig. 1) is based on a bulk heterojunction (BHJ)<sup>9,10</sup> active layer in which electron donor and acceptor components should form a bicontinuous composite of donor (usually a polymer) and acceptor (a fullerene derivative)

<sup>1</sup> R. Gaudiana, Third-Generation Photovoltaic Technology – The Potential for Low-Cost Solar Energy Conversion. *J. Phys. Chem. Lett.* **2010**, *1*, 1288-1289.

<sup>2</sup> R. Po, M. Maggini and N. Camaioni, Polymer Solar Cells: Recent Approaches and Achievements. *J. Phys. Chem. C* **2010**, *114*, 695-706.

<sup>3</sup> To Cap off a Magnificent Year, Solarmer Achieves 7.9% NREL Certified Plastic Solar Cell Efficiency. Press release, Solarmer Energy, Inc.: El Monte, CA, December 1, 2009.

<sup>4</sup> Y. Liang, Z. Xu, J. Xia, S.-T. Tsai, Y. Wu, G. Li, C. Ray, and L. Yu, For the Bright Future – Bulk Heterojunction Polymer Solar Cells with Power Conversion Efficiency of 7.4%. *Adv. Mater.* **2010**, *22*, E135-E138.

<sup>5</sup> G. Dennler, M. C. Scharber and C. J. Brabec, Polymer-Fullerene Bulk Heterojunction Solar Cells. *Adv. Mater.* **2009**, *21*, 1-16.

<sup>6</sup> J. Peet, A. J. Heeger and G. C. Bazan, “Plastic” Solar Cells: Self Assembly of Bulk Heterojunction Nanomaterials by Spontaneous Phase Separation. *Acc. Chem. Res.* **2009**, *42*, 1700-1708.

<sup>7</sup> S.R. Forrest, The Limits to Organic Photovoltaic Cell Efficiency, *MRS Bulletin*, **2005**, *30*, 28-32.

<sup>8</sup> J.Y. Kim, K. Lee, N. E. Coates, D. Moses, T.-Q. Nguyen, M. Dante and A. J. Heeger, Efficient Tandem Polymer Solar Cells Fabricated by All-Solution Processing. *Science* **2007**, *317*, 222-225.

<sup>9</sup> B. C. Thompson and J. M. J. Fréchet, Polymer-fullerene composite solar cells. *Angew. Chem. Int. Ed.* **2008**, *47*, 58-77.

<sup>10</sup> S. Günes, H. Neugebauer and N. S. Sariciftci, Conjugated Polymer Based Organic Solar Cells. *Chem. Rev.* **2007**, *107*, 1324-1338.

with a maximum interfacial area for exciton dissociation and a mean domain size commensurate with the exciton diffusion length. The two components should phase-segregate on a suitable length scale to allow maximum ordering within each phase and thus enable effective charge transfer along continuous pathways to the electrodes<sup>9</sup>.

In bulk heterojunction (BHJ) OPV devices, a donor-acceptor phase separation in a 10 to 20 nm length scale<sup>9,10,11</sup> together with improved phase separation and crystallinity are thought to be best for optimized performance<sup>9,10,15,16,18</sup>. Significant efforts to improve the morphology of active layers, for instance by annealing and the use of different and/or bi-component solvent systems for deposition, have been instrumental in achieving recent impressive performance improvements<sup>12,13,14,15</sup> and have been supported by increasingly sophisticated characterization techniques<sup>16</sup>. For instance, the three-dimensional nanoscale organization in common poly(3-hexylthiophene) (P3HT)/[6,6]-phenyl-C<sub>61</sub>-butyric acid methyl ester (PCBM) photoactive layers has been revealed by electron tomography<sup>17</sup> and the spatial distribution of photocurrent determined by means of photoconductive atomic force microscopy (pcAFM) and time-resolved electrostatic force microscopy (trEFM)<sup>18</sup>.

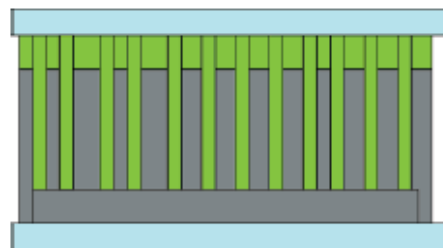


**Fig. 2** Ideal structure of an ordered heterojunction solar cell (taken from <sup>10</sup>)

The concept of an ordered heterojunction has recently been introduced<sup>10</sup> and is thought to be an ideal structure for the further development of heterojunction solar cells (shown schematically in Fig. 2). The two phases of donor and acceptor within the heterojunction are interspaced with an average length scale of approximately 10 to 20 nm, i.e., equal to or less than the exciton diffusion length. The two phases have to be interdigitated in percolated pathways to ensure high mobility charge carrier transport while minimizing recombination<sup>10,16</sup>. This can be achieved by increasing the mesoscopic order and crystallinity of the active layer, including concentration gradients of both the n- and p-phases<sup>10,16</sup>. The challenge is to generate a nanoscale interpenetrating network with a maximized interface between donor and acceptor materials

<sup>11</sup> M. C. Scharber, D. Mühlbacher, M. Koppe, P. Denk, C. Waldauf, A. J. Heeger and C. J. Brabec, Design rules for donors in bulk-heterojunction solar cells – towards 10% energy conversion efficiency. *Adv. Mater.* **2006**, *18*, 789-794.

<sup>12</sup> H. Hoppe and N. S. Sariciftci, Morphology of polymer/fullerene bulk heterojunction solar cells. *J. Mater. Chem.* **2006**, *16*, 45-61.

<sup>13</sup> A. J. Moulé and K. Meerholz, Controlling Morphology in Polymer-Fullerene Mixtures. *Adv. Mater.* **2008**, *20*, 240-245.

<sup>14</sup> J. Peet, J. Y. Kim, N. E. Coates, W. L. Ma, D. Moses, A. J. Heeger and G. C. Bazan, Efficiency enhancement in low-bandgap polymer solar cells by processing with alkane dithiols. *Nature Materials* **2007**, *6*, 497-500.

<sup>15</sup> J. K. Lee, W. L. Ma, C. J. Brabec, J. Yuen, J. S. Moon, J. Y. Kim, K. Lee, G. C. Bazan and A. J. Heeger, Processing additives for improved efficiency from bulk heterojunction solar cells. *J. Am. Chem. Soc.* **2008**, *130*, 3619-3623.

<sup>16</sup> R. Giridharagopal and D. S. Ginger, Characterizing Morphology in Bulk Heterojunction Organic Photovoltaic Systems. *J. Phys. Lett.* **2010**, *1*, 1160-1169.

<sup>17</sup> S. S. van Bavel, E. Sourty, G. de With and J. Loos, Three-dimensional nanoscale optimization of bulk heterojunction polymer solar cells. *Nano Lett.* **2009**, *9*, 507-513.

<sup>18</sup> C. Groves, O. G. Reid and D. S. Ginger, Heterogeneity in Polymer Solar Cells: Local Morphology and Performance in Organic Photovoltaics Studied with Scanning Probe Microscopy. *Acc. Chem. Res.* **2010**, *43*, 612-620.

within the whole volume of the photoactive layer for maximum photon absorption, exciton dissociation, and to ensure the creation of continuous, sufficiently short pathways for charge transport.

Recent examples of the ordered-heterojunction concept have included the addition of ionic structural units (ionomers) such as partially sulfonated polystyrene (PSP)<sup>19</sup>, the use of inorganic templates leading to nanorod arrays<sup>20</sup>, nanowires<sup>21</sup>, and one-dimensional nanostructures<sup>22</sup>.

The present Phase I work has focused on a similar increased ordering of the active layer by the use of inert silica spheres bonded to suitable fullerene derivatives. We have successfully demonstrated the concept with this project, meeting major requirements for necessary performance improvements:

- A higher degree of photon absorption is enabled by increased light scattering within the active layer.
- A maximized interface between electron donor and acceptor ensures efficient exciton dissociation.
- Discrete and highly ordered pathways lead to high electron and hole mobility. The resulting increased short-circuit current density will allow for thicker active layers and subsequent increased light scattering.

This work is complementary to the optimization of electron donor and acceptor electronic structures, allowing for the most efficient light absorption and highest voltage. The latter can be maximized by increasing the gap between the HOMO level of the electron donor and the LUMO level of the electron acceptor whereas low-bandgap polymers, which are currently in development, have large absorption coefficients at suitable wavelengths allowing for best energy absorption<sup>5,9,10,23,24,25</sup>. Actively pursued at Nano-C<sup>26,27</sup>, suitable chemical functionalization has

---

<sup>19</sup> K. C. Kim, J. H. Park and O. O. Park, New Approach for Nanoscale Morphology of Polymer Solar Cells. *Sol. Energy Mater. Sol. Cells* **2008**, *92*, 1188-1191.

<sup>20</sup> H.-S. Wang, L.-H. Lin, S.-Y. Chen, Y.-L. Wang and K.-H. Wei, Ordered Polythiophene/Fullerene Composite Core-Shell Nanorod Arrays for Solar Cell Applications. *Nanotechnology* **2009**, *20*, 1-5.

<sup>21</sup> H. Xin, O. G. Reid, G. Ren, F. S. Kim, D. S. Ginger and S. A. Jenekhe, Polymer Nanowire/Fullerene Bulk Heterojunction Solar Cells: How Nanostructure Determines Photovoltaic Properties. *ACS Nano* **2010**, *4*, 1861-1872.

<sup>22</sup> T. Sagawa, S. Yoshikawa and H. Imahori, One-Dimensional Nanostructured Semiconducting Materials for Organic Photovoltaics. *J. Phys. Chem. Lett.* **2010**, *1*, 1020-1025.

<sup>23</sup> N. Blouin, A. Michaud, D. Gendron, S. Wakim, E. Blair, R. Neagu-Plesu, M. Belletête, G. Durocher, Y. Tao and M. Leclerc, Toward a rational design of poly(2,7-carbazole) derivatives for solar cells. *J. Am. Chem. Soc.* **2008**, *130*, 732-742.

<sup>24</sup> A. B. Tamayo, B. Walker and T.-Q. Nguyen, A low band gap, solution processable oligothiophene with a diketopyrrolopyrrole core for use in organic solar cells. *J. Phys. Chem. C* **2008**, *112*, 11545-11551.

<sup>25</sup> Y. Liang, Y. Wu, D. Feng, S.-T. Tsai, H.-J. Son, G. Li and L. Yu, Development of new polymers for high-performance solar cells. *J. Am. Chem. Soc.* **2009**, *131*, 56-57.

<sup>26</sup> D. W. Laird, R. Stegamat, M. Daadi, H. Richter, V. Vejins, L. Scott and T. A. Lada, Organic Photovoltaic Devices Comprising Fullerenes and Derivatives thereof. US Patent Application, Pub No.: 2008/0319207 A1, Pub. Date: December 25, 2008.

<sup>27</sup> D. W. Laird, H. Richter, V. Vejins, L. Scott and T. A. Lada, Organic Photovoltaic Devices Comprising Fullerenes and Derivatives thereof and Improved Methods of Making Fullerene Derivatives. US Patent Application, Pub. No.: 2009/0176994 A1, Pub Date: July 9, 2009.

been demonstrated to be an efficient pathway to less negative LUMO levels and therefore higher voltage<sup>28,29,30</sup>. However, while further multiple functionalization beyond two functional groups has shown increased open circuit voltage, short circuit current dropped drastically, sacrificing overall device performance<sup>31</sup>. Morphology control, as developed here, may overcome this limitation and therefore enable the further optimization of voltage, current and absorption.

As fully described in more detail below, fullerene derivatives are either physically adsorbed or chemically bonded to inert silica (SiO<sub>2</sub>) nanospheres to form the n-phase of the active layer (Inorganic Core-Fullerene Shell (IC-FS) geometry). Such silica nanospheres are commercially available with well defined monodispersed size distributions of 10 nm and larger<sup>32,33</sup>. The electronic structure (particularly the LUMO level) of the n-phase, which is closely linked to the open circuit voltage, is set by the selection of the chemical functionalization through which the fullerene is attached to the silica surface. Additional functionalization of the fullerenes allows for further tuning of the electronic structure. Photoactive layers (as p-phase + n-phase inks) are prepared by mixing P3HT or other electron-donating polymers with the IC-FS. When deposited and dried, the resulting structure is a nano-composite active layer that provides an enhanced p/n interface.

Methods for fullerene derivatization, chemical bonding of the fullerene to the silica nanospheres, and p-n ink preparation have been developed at Nano-C. During this Phase I SBIR, device fabrication has been conducted by the team of Drs. Teresa Barnes and Dana Olson at the National Renewable Energy Laboratory (NREL) allocating 50% of the time of an experienced postdoc (Dr. Michael Woodhouse) to the project. The feasibility of the IC-FS concept was demonstrated and further refinement is expected to allow for a significant improvement of device performance, necessary for large scale commercialization. For instance, yields of the chemical functionalization of silica spheres need to be optimized and the degree of coverage on the silica surface controlled. The effect of the covalent bonding on electronic properties has to be better understood and methods for their control further developed. In so doing, the IC-FS concept has the potential to create a profound effect on OPV device performance and to lead to high-efficiency with long-term stability.

---

<sup>28</sup> F. B. Kooistra, J. Knol, F. Kastenberg, L. M. Popescu, W. J. H. Verhees, J. M. Kroon and J. C. Hummelen, Increasing the Open Circuit Voltage of Bulk-Heterojunction Solar Cells by Raising the LUMO Level of the Acceptor. *Org. Lett.* **2007**, *9*, 551-554.

<sup>29</sup> M. Lenes, G.-J. A. H. Wetzelaer, F. B. Kooistra, S. C. Veenstra, J. C. Hummelen and P. W. M. Blom, Fullerene Bisadducts for Enhanced Open-Circuit Voltages and Efficiencies in Polymer Solar Cells. *Adv. Mater.* **2008**, *20*, 2116-2119.

<sup>30</sup> Y. He, H.-Y. Chen, J. Hou and Y. Li, Indene Bisadduct: A New Acceptor for High-Performance Polymer Solar Cells. *J. Am. Chem. Soc.* **2010**, *132*, 1377-1382.

<sup>31</sup> M. Lenes, S. W. Shelton, A. B. Sieval, D. F. Kronholm, J. C. Hummelen and P. W. M. Blom, Electron Trapping in Higher Adduct Fullerene-Based Solar Cells. *Adv. Funct. Mater.* **2009**, *19*, 3002-3007.

<sup>32</sup> Microspheres-Nanospheres, Cold Spring, NY 10516, [www.microspheres-nanospheres.com](http://www.microspheres-nanospheres.com)

<sup>33</sup> <http://www.nissanchem-usa.com/organosilicasol.php>

## 2. Description of conducted work

Work conducted at Nano-C and NREL during this project has convincingly demonstrated the compatibility of silica spheres with the good functioning of bulk heterojunction OPV devices. While methodology allowing for the efficient and controlled covalent bonding of fullerenes on the surface of silica spheres has been developed, OPV performance of non-covalently bonded

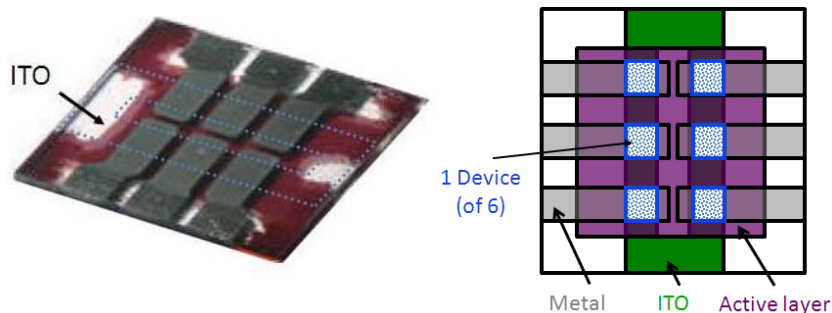


**Fig. 3** Example of set of six devices built at NREL: a) Photograph and b) Schematic of the design. Each device covers  $0.11 \text{ cm}^2$ .

mixtures between [6,6]-phenyl- $\text{C}_{61}$ -butyric acid methyl ester (PCBM) and silica spheres with average diameters of 10 to 15 nm combined with P3HT have been investigated. For this purpose, silica spheres rendered soluble in toluene by limited functionalization and commercially available<sup>33</sup> have been used. Active layers have been deposited by means of spin coating as described in the literature<sup>34</sup>. A picture of the resulting device and an explanatory schematic are shown in Fig. 3. Briefly, patterned indium tin oxide (ITO) substrates are first mechanically cleaned and sonicated sequentially in acetone and isopropyl alcohol, before being blown dry with  $\text{N}_2$ . The substrates are then exposed to an oxygen plasma. Next, a hole injection layer of poly(3,4-ethylenedioxythiophene)poly(styrenesulfonate) (PEDOT:PSS, Baytron P VP AI 4083, filtered through  $0.45 \mu\text{m}$ ) is spin coated twice and baked on a hotplate at  $120 \text{ }^\circ\text{C}$  for 1 h. The sample is then transferred to a glovebox for all subsequent deposition and characterization steps.

Typically, the active layers are prepared from 1:1 blends of, e.g., poly(3-hexylthiophene) (P3HT) and [6,6]-phenyl  $\text{C}_{61}$ -butyric acid methyl ester (PCBM) dissolved in toluene or *o*-

**Table 1** Characteristics of bulk heterojunction devices using P3HT as p-phase and PCBM-silica mixtures as n-phase.

PCBM : silica ratio	$V_{oc}$ (V)	$J_{sc}$ ( $\text{mA cm}^{-2}$ )	Fill Factor	Efficiency (%)
1:0 (baseline)	$0.573 \pm 0.01$	$5.85 \pm 0.06$	$43.97 \pm 2.50$	$1.41 \pm 0.09$
6.14:1	$0.581 \pm 0.002$	$5.95 \pm 0.18$	$52.05 \pm 2.69$	$1.73 \pm 0.08$
3:1	$0.584 \pm 0.003$	$5.65 \pm 0.21$	$50.44 \pm 2.07$	$1.71 \pm 0.08$

dichlorobenzene. The solutions are stirred on a hotplate at  $60 \text{ }^\circ\text{C}$  for at least 24 hours prior to deposition. The active layer is deposited by spin coating to achieve the optimal active layer thickness of 250-300 nm. Each sample is placed in a covered petri dish for at least 1 h to slowly dry, enhancing the film morphology. After drying, the samples are baked at  $110 \text{ }^\circ\text{C}$  for 10 min

<sup>34</sup> Reese, M. O.; White, M. S.; Rumbles, G.; Ginley, D. S.; Shaheen, S. E., Optimal negative electrodes for poly(3-hexylthiophene): [6,6]-phenyl  $\text{C}_{61}$ -butyric acid methyl ester bulk heterojunction photovoltaic devices. *Appl. Phys. Lett.* **2008**, 92, (5), 053307-3.

before being transferred to the evaporation chamber. Layers of Ca and Al of 20 nm and 100 nm thicknesses, respectively, are then thermally evaporated to form the back contact.

In order to assess the effect of silica spheres on film morphology and subsequent performance,

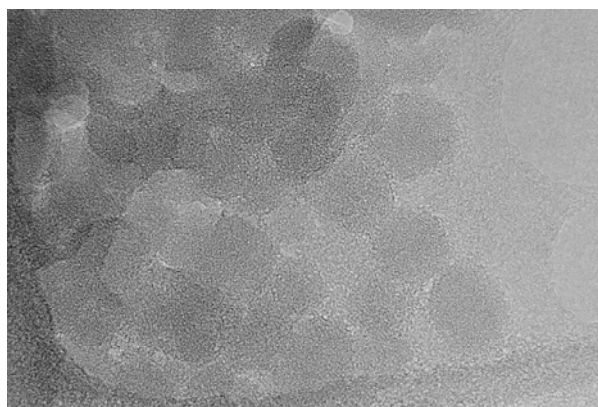


**Fig. 4** TEM image of PCBM/silica/P3HT mixture.

ratios between PCBM and silica spheres of 6.14:1, 3:1, 1:1 and 1:3 were studied. As silica spheres are not active electron acceptors, toluene solutions containing 10 mg/mL of PCBM were prepared in all cases. 20 mg of P3HT were added to 2 mL aliquots of these solutions and devices prepared maintaining a 1-to-1 PCBM:P3HT ratio. In addition, a PCBM:P3HT device, without the presence of any silica spheres, was prepared as a baseline. After an initial screening, six devices each, covering 0.11 cm<sup>2</sup> respectively, were prepared for the baseline as well as 6.14:1 and 3:1 PCBM-silica ratios. Standard deviations were determined. A TEM image of a PCBM/silica/P3HT mixture is shown in Fig. 4 confirming the presence of particles with diameters between approximately 12 and 14 nm. First AFM measurements in order to assess differences in morphology have been conducted but additional measurements are required for definitive conclusions.

As shown in Table 1 and illustrated in the I-V curves given in Fig. 5, statistically meaningful improvements of performance of >20% compared to the PCBM:P3HT base case could be achieved using PCBM:silica spheres in 6.14:1 and 3:1 mixtures. Significant further improvements are likely to be possible as no optimization of critical process parameters, such as the p-phase/n-phase ratio, the annealing temperature or, particularly, the solvent system, was conducted. For instance, an approximately two-fold increase in performance by preparing the active layer in chlorobenzene instead of toluene has been reported previously for PCBM-based cells<sup>35</sup>, indicating the potential of significant further improvements.

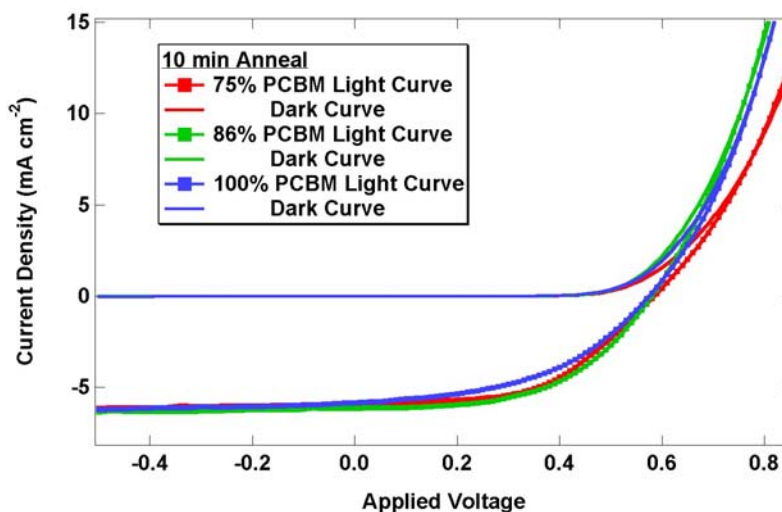


**Fig. 5** I-V curves of bulk heterojunction devices based on a) PCBM:P3HT, b) PCBM (86%)/silica (14%): P3HT and c) PCBM (75%)/silica (25%): P3HT.

<sup>35</sup> S. E. Shaheen, C. J. Brabec, N. S. Sariciftci, F. Padinger, T. Fromherz and J. C. Hummelen, 2.5% Efficient Organic Plastic Solar Cells. *Appl. Phys. Lett.* **2001**, 78, 841-843.

Covalent bonding of fullerenes to silica spheres was found to be challenging, mainly because of the lack of solvents suitable for both silica spheres and fullerene derivatives. First experiments

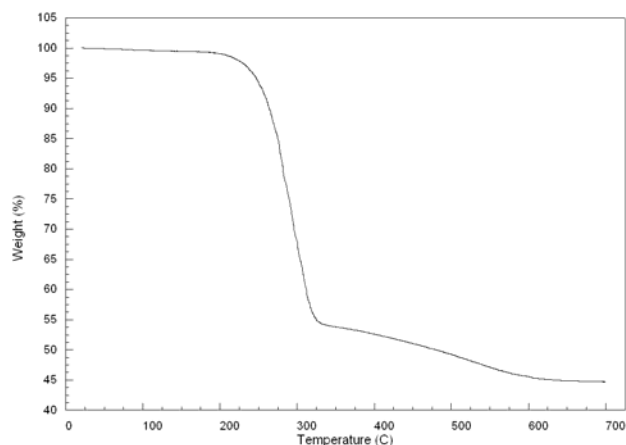


**Fig. 6** Thermogravimetric analysis (TGA) under air of covalently bonded PCBM-silica. Heat rate: 7.5 K/min.

techniques and the use for device fabrication was hampered by the lack of solubility in any common solvent.

Accordingly, functionalization was conducted using a commercially available toluene solution of –OH-bearing silica spheres with particle diameters between 10 and 15 nm, rendered soluble by limited functionalization<sup>33</sup> (this same material was used in the above-reported investigation as the silica additive to PCBM:P3HT devices).

Initial experiments with this material attempted to form an ester linkage between PCBM and silica using an acid or base catalyzed mechanism; however, this method provided limited yield and reproducibility. As such, a transesterification method, previously developed at Nano-C<sup>37</sup>, was successfully adapted for this project. The use of di-n-butyltin oxide as the catalyst leads to the formation of Si-O-CO-R ester functionalities in harvestable yields and with significant reproducibility. The reaction was conducted in o-dichlorobenzene at 80 °C under nitrogen, allowing for higher concentrations of the reactants, particularly PCBM, and therefore reaction rates.

Analysis by HPLC using a silica gel chemically bonded with 3-(1-pyrenyl)propyl (Buckyprep, Nacalai USA, Inc.<sup>38</sup>) with toluene as the eluent showed the time-dependent growth of a new peak

were conducted with commercially available water-based solutions of either –OH bearing or amino-functionalized silica spheres having a diameter of 10 nm<sup>32</sup>. Initial attempts to form ester (-O-CO-CH<sub>2</sub>-) or amide (-NH-CO-CH<sub>2</sub>-) bonds using [6,6]-phenyl-C<sub>61</sub>-butyric acid (PCBA)<sup>36</sup>, carrying a carboxylic acid end group had only limited success. While IR spectroscopy and transmission electron microscopy (TEM) imaging showed some evidence of successful functionalization, further characterization suggested the presence of a silica-PCBM mixture instead of a covalently bonded new compound. In addition, purification by means of chromatographic

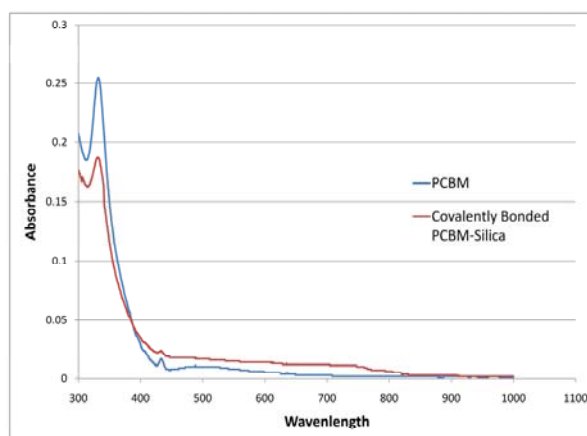


**Fig. 7** UV-vis spectrum of a) unfunctionalized silica spheres and b) covalently bonded PCBM-silica.

<sup>36</sup> J. C. Hummelen, B. W. Knight, F. LePeq and F. Wudl, Preparation and Characterization of Fulleroid and Methanofullerene Derivatives. *J. Org. Chem.* **1995**, *60*, 532-538.

<sup>37</sup> D. F. Kronholm, J. C. Hummelen and A. B. Sieval, High-Efficiency Fullerene-Based Radical Scavengers. US Patent Application, Appl. No.: 11/014,115, December 15, 2004.

<sup>38</sup> <http://www.nacalaiusa.com/product.php?cmd=hplc>

eluting between those of unreacted silica spheres and PCBM. Analysis by HPLC on a conventional unfunctionalized silica stationary phase indicated the growth of three new peaks after the characteristic PCBM one. Once the reaction completed, purification by means of column chromatography using 15 micron reverse phase silica proved unsuccessful. However, a usable purification method was finally identified in the form of a 40-60 micron silica bed using *o*-dichlorobenzene as the eluent. This process resulted first in the recovery of unreacted PCBM followed by two distinguished bands.

Thermogravimetric analysis (TGA) under air confirmed the presence of both organic and inorganic, non-oxidizing material in the reaction mixture. The largest non-PCBM fraction collected during chromatography (~200 mg), was found to be the most soluble in toluene (>20

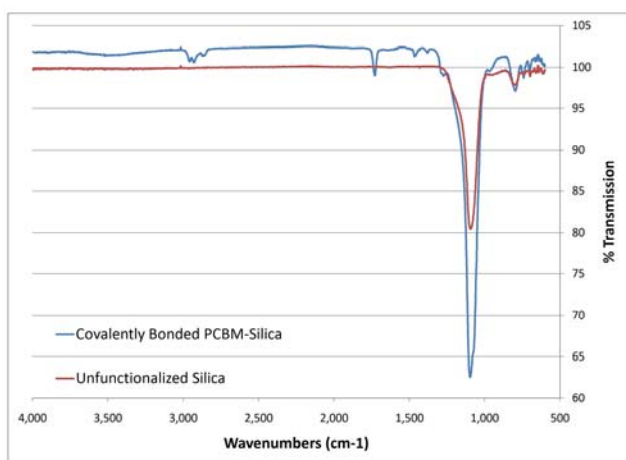


**Fig. 8** Infrared spectrum of a) unfunctionalized silica spheres and b) covalently bonded PCBM-silica.

mg/mL) as well as *o*-dichlorobenzene (>16 mg/mL) and was further analyzed in some detail. TGA of this material, given in Fig. 6, shows oxidation of material (probably the PCBM functionality) at 250 °C representing approximately 45% of the total mass, followed by an additional 10% gradual weight loss. Comparison with the TGA of the unfunctionalized toluene-soluble silica spheres shows a similar 10% weight loss, most likely explained by the functional groups added in the commercial product in order to achieve solubility. As the TGA plot given in Fig. 6 is significantly different from those of unfunctionalized silica spheres and PCBM (wherein oxidation starts at approximately 475 °C), the presence of a simple silica-PCBM mixture without covalent bonding can be excluded. The UV-vis spectrum of the toluene solution has been measured and its pronounced similarity to the corresponding PCBM spectrum (Fig. 7) is in agreement with the very limited absorbance of silica in this part of the electromagnetic spectrum meaning that silica does not contribute to the absorption spectrum in the range of wavelengths scanned here. This similarity of the UV-vis spectra confirms the expectation that covalent attachment of PCBM to silica far from the most absorbing fullerene cage does not significantly affect the electronic structure.

Further confirmation of the composition of the collected product has been obtained by IR spectroscopy. Comparison of unfunctionalized silica spheres and the reaction product (Fig. 8) shows the presence of silanol Si-O stretches (~940  $\text{cm}^{-1}$ ) and Si-O-Si asymmetric stretches (1200 to 1000  $\text{cm}^{-1}$ ) in both spectra while saturated carbonyl (C=O) stretches (~1729  $\text{cm}^{-1}$ ) and asymmetric (2920 to 2970  $\text{cm}^{-1}$ ) C-H stretches, consistent with the PCBM spectrum which shows peaks at ~2960  $\text{cm}^{-1}$  as well as 1736  $\text{cm}^{-1}$  on this instrument, can only be observed with the covalently bonded PCBM-silica sample. In addition, an IR band around 1430  $\text{cm}^{-1}$  is in agreement with the presence of  $\text{C}_{60}$  fullerene as a structural unit<sup>39</sup> (the other characteristic  $\text{C}_{60}$  stretch at 1180  $\text{cm}^{-1}$  is likely overshadowed by the strong Si-O-Si stretch). It can therefore be

<sup>39</sup> W. Krätschmer, L. D. Lamb, K. Fostiropoulos and D. R. Huffman, Solid  $\text{C}_{60}$ : A New Form of Carbon. *Nature* **1990**, *347*, 354-358.

concluded that the synthesis of Inorganic Core-Fullerene Shell (IC-FS), i.e., of covalently bonded fullerene-silica compounds, was successful.

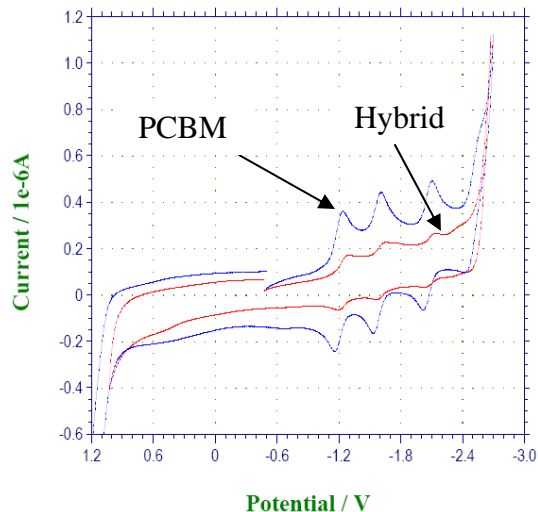


**Fig. 9** CV trace of a) PCBM-functionalized silica spheres (hybrid) and b) plain PCBM.

Additional characterization, for instance by means of cyclic voltammetry (CV) and transmission electron microscopy (TEM) has been conducted. The CV trace of PCBM-functionalized silica spheres (hybrid) was compared with that of plain PCBM (Fig. 9). While very similar characteristics were seen, reductions for the hybrid are shifted to a slightly more negative potential than plain PCBM.

A sample has been shipped to NREL and first devices resulting from covalently bonded PCBM-silica dissolved in toluene together with P3HT and then deposited by spin coating have been prepared. While photodiode behavior with a voltage slightly lower than that of plain PCBM (consistent with the CV trace) was observed, further optimization of the device fabrication is needed to achieve photocurrents at the required level. Other important steps in future work will also include additional purification of the PCBM-functionalized silica spheres.